Articles

Loop Mobility in a Four-Helix-Bundle Protein: ^{15}N NMR Relaxation Measurements on Human Interleukin-4†

Christina Redfield,‡ Jonathan Boyd,‡ Lorna J. Smith,‡ Richard A. G. Smith,§ and Christopher M. Dobson*,‡

Inorganic Chemistry Laboratory and Department of Biochemistry, University of Oxford, South Parks Road, Oxford OX1 3QR, England, and SmithKline Beecham Pharmaceuticals, Great Burgh, Yew Tree Bottom Road, Epsom, Surrey KT18 5XQ, England

Received June 22, 1992; Revised Manuscript Received July 30, 1992

ABSTRACT: ^{15}N NOE, T_1, and T_2 measurements have been carried out on uniformly ^{15}N-labeled human interleukin-4. Analysis of the results in terms of order parameters (S^2) shows that although the helical core of this four-helix-bundle protein exists as a well-defined structure with limited conformational flexibility ($S^2 \simeq 0.9$), other regions of the molecule experience substantial fluctuations in the conformation of the main chain ($S^2 = 0.3$–0.8). These regions include both the N- and C-termini and two of the loops joining the helices. The majority of these internal motions are fast compared with the overall rotational correlation time ($\tau_R = 7.6$ ns at 35 °C) and are localized in regions that are relatively ill-defined in the NMR structures previously determined for this protein [Smith, L. J., Redfield, C., Boyd, J., Lawrence, G. M. P., Edwards, R. G., Smith, R. A. G., & Dobson, C. M. (1992) *J. Mol. Biol. 224*, 899–904]. Other motions are on a slower time scale and appear to be associated with two of the three disulfide bonds and the β-sheet region in the protein. The dynamic properties of interleukin-4 in solution have been compared with features of the X-ray structures of other four-helix-bundle proteins. The results suggest that the dynamic properties observed here may be general for this class of proteins and may be significant for the interpretation of both their structural and functional properties.

We have recently reported the structure of human interleukin-4 (Redfield et al., 1991; Smith et al., 1992), one of the group of helical cytokines which modulate cell proliferation and differentiation within the immune system. IL-4[1] is of particular interest as the regulator of IgE and low-affinity IgE receptor production and for its role in the generation of cytotoxic T-cells (Howard et al., 1982; De France et al., 1987a,b; Vercelli et al., 1989). The structure was determined in solution using NOE and coupling constant data derived from 2-D and 3-D NMR experiments carried out on a singly-labeled ^{15}N sample and a doubly-labeled ^{13}C-^{15}N sample of recombinant IL-4, both produced in *Escherichia coli*. It comprises a four-helix bundle in a left-handed up–up–down–down topology and a small section of irregular antiparallel β-sheet; the structure is shown schematically in Figure 1A. Essentially the same structure has recently been identified in a modified recombinant IL-4 derived from yeast (Garrett et al., 1992; Powers et al., 1992). A closely similar structure has been found from X-ray diffraction studies of crystals of granulocyte macrophage-colony stimulating factor (GM-CSF) (Diederichs et al., 1991). Both IL-4 and GM-CSF have the same overall helix-bundle topology as growth hormone (Abdel-Meguid et al., 1987) but differ in the orientation of the loop regions. Despite their similar topologies the primary sequences of the four-helix-bundle cytokines show little homology.

A striking feature of the interleukin-4 solution structure is that the core of the molecule is much better defined than the loops that link the helices together (Smith et al., 1992). Thus, the rmsd between C^α positions in the family of NMR structures is 0.56 Å for the four-helix core but 1.41 Å overall with values of 2.0 Å or more in the loops and termini. These large rmsd values are primarily a consequence of the small number of long-range NOE restraints for these regions. Whether this arises because such effects have not yet been assigned in the spectrum, for example, because of overlap, or because dynamic disorder exists in these regions of the structure cannot be deduced from the information used to define the structures. NMR relaxation studies, however, can provide direct information about molecular dynamics in solution. In particular, ^{15}N NOE, T_1, and T_2 measurements are able to probe protein backbone motions at the level of individual residues (Kay et al., 1989; Clore et al., 1990b). In this paper we report such measurements for interleukin-4 and show that they provide considerable insight into the behavior of the different regions of the molecular structure.

MATERIALS AND METHODS

Collection of ^{15}N NMR Relaxation Data. The preparation of uniformly ^{15}N-labeled human interleukin-4 was carried out as described previously (Redfield et al., 1991). The NMR

† Contribution from the Oxford Centre for Molecular Sciences, which is supported by the U.K. Science and Engineering Research Council and the Medical Research Council.

* To whom correspondence should be addressed at the Inorganic Chemistry Laboratory, University of Oxford.

‡ University of Oxford.

§ SmithKline Beecham Pharmaceuticals.

[1] Abbreviations: IL-4, human interleukin-4; NMR, nuclear magnetic resonance; NOE, nuclear Overhauser enhancement; rmsd, root-mean-square deviation; T_1, spin–lattice relaxation time; T_2, spin–spin relaxation time; GM-CSF, granulocyte macrophage-colony stimulating factor; S^2, order parameter; S^2_f, order parameter for fast time-scale motion; S^2_s, order parameter for slow time-scale motion; τ_R, rotational correlation time; τ_e, effective correlation time for internal motion; τ_s, effective correlation time for slow time-scale internal motion; τ_f, effective correlation time for fast time-scale internal motion.

0006-2960/92/0431-10431$03.00/0

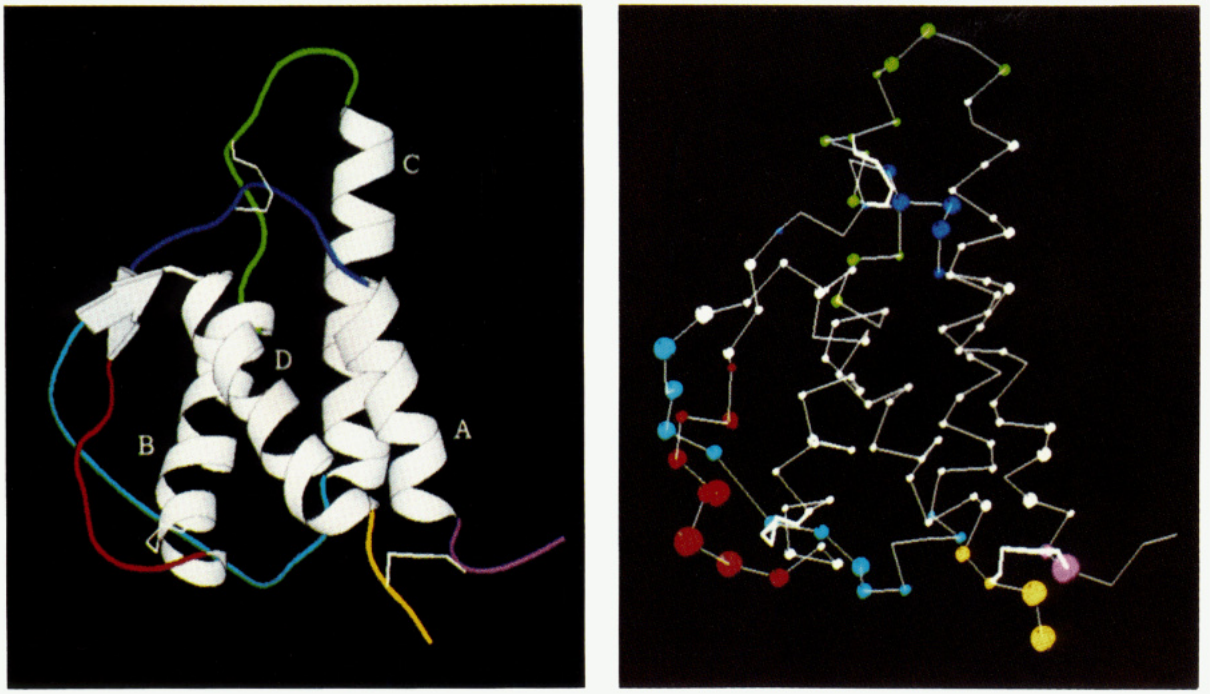

FIGURE 1: (A, left) Ribbon diagram of the average calculated solution structure of IL-4 showing the main-chain fold and the elements of secondary structure. The helices and β-sheet are shown in white. The N- and C-termini and the AB1, AB2, BC, and CD loops are shown in purple, yellow, dark blue, red, green, and cyan, respectively. The four helices are labeled. (B, right) C^{α} trace of the backbone of IL-4. The diameter of the balls represents the S^2 values found for each amino acid residue; a small ball represents a large S^2 value, and a large ball represents a small S^2 value. Seven different diameters representing S^2 values of 0.30–0.39, 0.40–0.49, 0.50–0.59, 0.60–0.69, 0.70–0.79, 0.80–0.89, and 0.90–1.0 have been used. No ball is drawn for residues for which S^2 was not determined. The color scheme is the same as in (a). The diagrams were generated using MOLSCRIPT (Kraulis, 1991).

experiments were performed on two home-built spectrometers, using GE/Nicolet software and digital control equipment, which operate at 360.1 and 500.1 MHz for ^{1}H and 36.5 and 50.7 MHz for ^{15}N. All NMR experiments were performed on a 2 mM sample of protein at pH 5.6 and 35 °C.

The pulse sequences for the ^{15}N longitudinal and transverse relaxation time measurements and the heteronuclear Overhauser experiment were based on the ^{1}H-detected ^{15}N–^{1}H correlation experiments originally described by Bodenhausen and Ruben (1980). The pulse sequences used to monitor the specific relaxation process, T_1, T_2, and NOE, have been described previously (Kay et al., 1989; Boyd et al., 1990; Palmer et al., 1992; Kay et al., 1992). Particular care was taken to remove the effects of cross-correlation between the two dominant relaxation mechanisms of the ^{15}N nucleus, those associated with dipolar coupling and chemical shift anisotropy, which could otherwise lead to a multiexponential decay process complicating the analysis of the restricted set of relaxation parameters reported here (Boyd et al., 1990, 1991; Palmer et al., 1992).

Sweep widths of 10869.56 and 1059.32 Hz were used in F_2 and F_1, respectively. A total of 2K complex data points were collected in F_2. Sign discrimination in F_1 was achieved using the method of States et al. (1982). The ^{1}H carrier was positioned on the H_2O resonance, and the ^{15}N carrier was positioned at 118.4 ppm. Measurements of the ^{15}N T_1 and T_2 values were carried out at 50.7 MHz. A series of 11 experiments with relaxation delays of 25, 75, 100, 150, 200, 300, 400, 600, 800, 1000, and 1200 ms were carried out for the measurement of T_1 using the pulse sequence described by Boyd et al. (1990). A recycle delay of 4 s was used and 96 complex t_1 increments of 16 scans were acquired. A series of eight experiments with relaxation delays of 8.6, 17.1, 34.2, 51.3, 68.4, 102.6, 136.8, and 205.2 ms were carried out for the measurement of T_2 using the pulse sequence described by Kay et al. (1992). A recycle delay of 2 s was used, and 128 complex t_1 increments of 32 scans were acquired. The delay between 180° pulses in the CPMG sequence (2τ) was set to 1 ms. In both sets of experiments water suppression was achieved using a combination of low-power solvent saturation and trim pulses (Messerle et al., 1989). The relaxation times T_1 and T_2 were obtained from exponential fits of the peak height data. NOE experiments were carried out at both 36.5 and 50.7 MHz using the pulse sequence described by Kay et al. (1989). In each case two spectra were collected, one with the NOE and one without. A recycle delay of 3.1 s was used, and 128 complex t_1 increments of 128 scans were acquired. In the experiment with the NOE, the ^{1}H spectrum was saturated by applying a nonselective 135° pulse every 8 ms for a period of 3 s. The solvent signal was suppressed using trim pulses (Messerle et al., 1989) for the NOE experiment performed at 50.7 MHz, but for that carried out at 36.5 MHz low-power solvent saturation was necessary in addition to the trim pulses. The NOE effect was calculated as the ratio of peak heights in spectra collected with and without NOE.

Analysis of ^{15}N NMR Relaxation Data. The ^{15}N relaxation data for interleukin-4 were analyzed using the formalism of Lipari and Szabo (1982a,b). Theoretical values for the T_1 and T_2 relaxation times and the NOE were calculated using the appropriate expressions (Abragam, 1961; Lipari & Szabo, 1982a,b), where S^2, S^2_s, S^2_f, τ_R, τ_e, and τ_s were used as previously defined (Lipari & Szabo, 1982a,b; Clore et al., 1990a). This model assumes that the molecule undergoes isotropic tumbling; the three principal components of the inertia tensor have been calculated from the average solution structure of IL-4 to be in a ratio of 1.81:1.46:1.00, indicating that IL-4 is a globular structure for which this should be a good approximation. A value for the rotational correlation time, τ_R, was obtained from analysis of the T_1/T_2 ratios for residues which did not show evidence of significant, fast

Table I: Summary of the Relaxation Data Analysis for Human Interleukin-4

T_1/T_2	NOE[a]	S^2_{av}[b]	$\pi\Delta$ex (s^{-1})	no. of residues	location			
					helix	sheet	loop	termini
4.92 ± 0.29[c]	≥0.75	0.93 ± 0.04		47	36	2	9	0
≤4.63[c]	≥0.75	0.84 ± 0.07		14	6	2	6	0
≥5.21[d]	≥0.75	0.90 ± 0.05	0.6–6.9	21	13	2	6	0
4.92 ± 0.29[e]	≤0.75	0.83 ± 0.10		5	1	0	2	2
≤4.63[f]	≤0.75	0.60 ± 0.16		20	3	0	13	4
≥5.21[g]	≤0.75	0.87 ± 0.08	1.3–11.2	3	0	0	3	0
≥5.21[h]	≤0.75	0.67 ± 0.05	3.2–5.0	3	0	0	3	0

[a] These values refer to the NOE measured at 50.7 MHz. The cutoff value for the NOE at 36.5 MHz was ~0.65. [b] All calculations were performed with a value of -156×10^{-6} for the difference in the parallel and perpendicular components of the axially symmetric ^{15}N chemical shift tensor ($\sigma_\parallel - \sigma_\perp$). This number is the average of several published values (Oas et al., 1987; Himaya et al., 1988; Shoji et al., 1990). An NH bond length of 1.02 Å (Keiter et al., 1986) was used in all calculations. This value has been used in most ^{15}N relaxation studies of proteins (Kay et al., 1989; Clore et al., 1990b; Schneider et al., 1992; Stone et al., 1992). The average S^2 value of ~0.90 observed in regions of secondary structure in IL-4 is somewhat higher than that observed in other studies of proteins (Kay et al., 1989; Clore et al., 1990b; Schneider et al., 1992; Stone et al., 1992). An NH bond length of 1.01 Å, recently used in the study of calmodulin (Barbato et al., 1992), gives an average S^2 value of ~0.87, which is more in line with that found in other studies. It should be noted, however, that while changes in the overall value used for the NH bond length will alter the absolute values obtained for S^2, they will not alter the trends observed. [c] Data were analyzed using a simplified version of the spectral density function where only S^2 is fitted. [d] Data were analyzed using the simplified version of the spectral density function with the addition of an extra relaxation contribution ($\pi\Delta$ex) in the expression for T_2. [e] Data were analyzed using the more general form of the spectral density function in which both S^2 and τ_e are fitted. The average value of τ_e for this group of residues was 42.6 ± 15.5 ps. [f] Data were analyzed using the extended model of Clore et al. (1990a) in which S^2_s, S^2_f, and τ_s are fitted. The average values of S^2_s, S^2_f, and τ_s were 0.75 ± 0.14, 0.79 ± 0.08, and 1.85 ± 0.73 ns, respectively. [g] Data were analyzed as in footnote *e* with the addition of $\pi\Delta$ex to account for exchange broadening. The average value of τ_e for this group of residues was 69.5 ± 46.4 ps. [h] Data were analyzed as in footnote *f* with the addition of $\pi\Delta$ex to account for exchange broadening. The average values of S^2_s, S^2_f, and τ_s for this group of residues were 0.80 ± 0.05, 0.83 ± 0.02, and 0.95 ± 0.38 ns, respectively.

motional averaging or exchange broadening; this ratio was found to be 4.92 ± 0.29 for 42 residues in helical regions, giving a τ_R of 7.56 ns. The procedures used to extract order parameters and correlation times for internal motions from the four measured relaxation parameters are described below and summarized in Table I.

The specific form of the spectral density function used in the analysis of the relaxation data for a particular residue depended on the values of the T_1/T_2 ratio and the NOE observed experimentally for that residue. The simplest form of the spectral density function which gave good agreement between the experimental and calculated values of T_1, T_2, and NOE for a particular residue was chosen. Residues with T_1/T_2 ratios of 4.92 ± 0.29 and with an NOE of greater than 0.75 at 50.7 MHz (≥0.65 at 36.5 MHz) were analyzed using a simplified version of the spectral density function (eq 9, Kay et al, 1989), which assumes that internal motions are of small amplitude ($S^2 \geq 0.7$) and are characterized by a τ_e that is very much faster than τ_R and, therefore, does not influence T_1 and T_2. The relaxation data for 47 residues meet these criteria and can be reproduced with a single parameter, S^2. The relaxation data for the 14 residues with T_1/T_2 ratios of less than 4.63 and an NOE of greater than 0.75 were also analyzed using this simplified model. Residues with T_1/T_2 ratios greater than 5.21 and with an NOE of greater than 0.75 at 50.7 MHz were analyzed using the simplified spectral density function with the addition of an extra relaxation contribution ($\pi\Delta$ex), modeling some form of conformational exchange broadening, in the expression for T_2; the relaxation data for 21 residues meet these criteria. The 31 remaining residues have an NOE of less than 0.75 at 50.7 MHz; these residues require a more complicated form of the spectral density function. The relaxation data for the five residues with T_1/T_2 ratios of 4.92 ± 0.29 and an NOE of less than 0.75 can be fitted satisfactorily using S^2 and τ_e (eq 4, Kay et al., 1989). The relaxation data for the 20 residues with T_1/T_2 ratios below 4.63 and an NOE of less than 0.75 cannot be fitted adequately using only S^2 and τ_e; values of these parameters which give a good fit for T_1 and T_2 lead to too low a value for the NOE at both 36.5 and 50.7 MHz. A similar situation has been found for a number of residues of staphylococal nuclease and interleukin-1β (Clore et al., 1990a). In these proteins the relaxation data could be accounted for if two internal motions faster than τ_R were assumed; one motion is very fast ($\tau_f \leq 10$ ps) and the second is at least 1 order of magnitude slower than τ_f ($\tau_s \simeq 1$ ns) (eq 14, Clore et al., 1990b). Application of this model to IL-4 results in good agreement between experimental and calculated T_1, T_2, and NOE values. The six remaining residues have T_1/T_2 ratios of greater than 5.21 and NOE values of less than 0.75; these represent a situation where T_2 exchange broadening increases the T_1/T_2 ratio and fast internal motion probably decreases the ratio (Clore et al., 1990b). The relaxation data for three of these residues requires fitting three parameters, S^2, τ_e, and $\pi\Delta$ex. The relaxation data for the remaining three residues requires fitting four parameters, S^2_s, S^2_f, τ_s, and $\pi\Delta$ex.

RESULTS AND DISCUSSION

The experimental NOE values and T_1/T_2 ratios are plotted against amino acid sequence in panels B and C of Figure 2, respectively. For the majority of residues, an NOE of greater than 0.75 at 50.7 MHz and 0.70 at 36.5 MHz is observed; these values require that any motions faster than τ_R are of small magnitude. There are, however, several regions of the protein backbone which show groups of residues with a significantly smaller NOE; this reflects a significant degree of rapid motion. The order parameters, S^2, derived from analysis of the relaxation data (Table I) are plotted against amino acid sequence in Figure 2D. For the majority of residues an order parameter of greater than 0.85 is observed. This value is comparable to those observed for backbone amides of compact protein structures (Kay et al., 1989; Clore et al., 1990b; Schneider et al., 1992; Stone et al., 1992) and is similar to values calculated from molecular dynamics simulations for well-defined internal residues in proteins (Olejniczak et al., 1984). There is, however, a substantial number of residues (23 out of 113) which show significantly smaller values of S^2 (≤0.75), indicative of motions of larger amplitude. Interleukin-4 appears to differ from many proteins whose dynamical properties have been studied by ^{15}N relaxation methods in both the number of residues showing such values and their distribution in distinct regions of the structure. Very recently, ^{15}N relaxation studies on calbindin D_{9k} (Kördel et al., 1992)

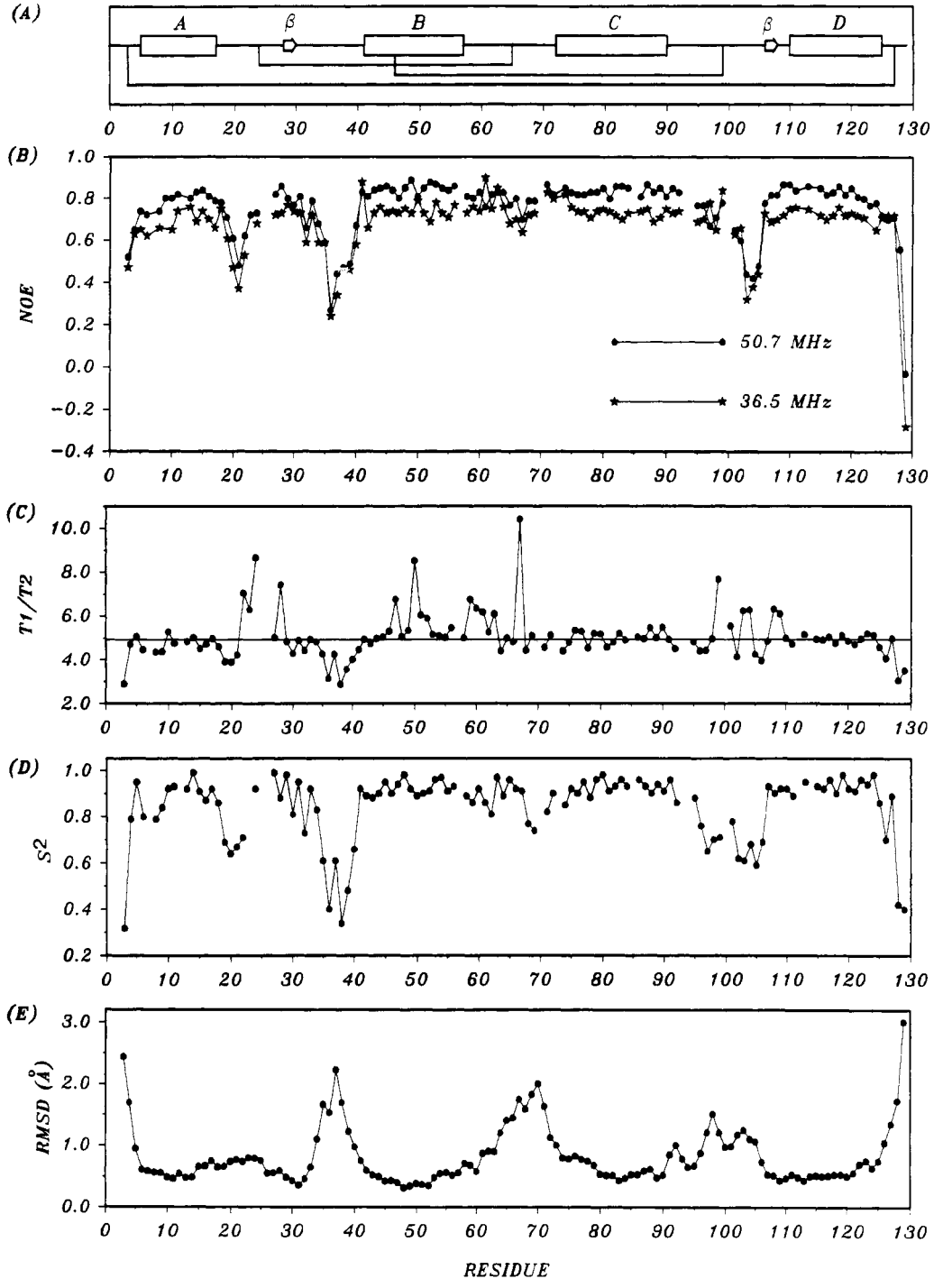

FIGURE 2: (A) Schematic representation of the secondary structure of IL-4. The rectangles and arrows represent helices and β-strands, respectively. The three disulfide bridges (3–127, 24–65, and 46–99) are indicated. (B) Plot of the observed ^{15}N NOE at 50.7 MHz (●) and 36.5 MHz (★) versus amino acid sequence. (C) Plot of the observed T_1/T_2 ratio versus amino acid sequence. The horizontal line at T_1/T_2 = 4.92 represents the average ratio used for the determination of the rotational correlation time. (D) Plot of the calculated S^2 value versus amino acid sequence. (E) Plot of the rmsd for N atom positions versus amino acid sequence. The rmsd values are between the 10 calculated solution structures and the restrained minimized average structure when the N, C^α, and C atoms of residues 3–127 are superimposed.

and calmodulin (Barbato et al., 1992) have identified regions of the structure which give low values of S^2 characteristic of rapid internal motions as has been found here for IL-4.

The distribution of S^2 values in terms of the structure of IL-4 is shown in Figure 1B. In Table II average values of S^2 for the different structural regions of the protein are shown; these values enable the overall pattern of behavior to be seen particularly clearly. The four helical regions of the protein have nearly identical values of the order parameter S^2; all residues within the helices have S^2 values of 0.79 or more. A larger range of S^2 values is observed among the residues of the β-sheet region, and the average order parameter found is somewhat lower than that observed for the helices. However, the central residues in the sheet, V29 and S107, have particularly high order parameters; these residues are involved in a pair of hydrogen bonds (NH29–CO107, NH107–CO29) which hold the two short strands of the sheet region together. The relaxation results reemphasize the significance of this structural feature, first identified in IL-4, for the overall architecture of this type of bundle.

The N- and C-terminal regions of the structure which precede and follow the A and D helices, respectively, have

Table II: Order Parameters (S^2), Amplitude of Motions (θ_0, ϕ_s, and $0.5\phi_s + \theta_0$), rmsd Values, and Angular Variations in Calculated Structures (Θ_{av}) for the Helical, β-Sheet, Loop, and Terminal Regions of Human Interleukin-4

	S^2_{av}	$\theta_{0\,av}$	$\phi_{s\,av}$	$(0.5\phi_s + \theta_0)_{av}$[a]	$rmsd_{av}$[b]	Θ_{av}[c]
helix A[d]	0.89 ± 0.06[e]	13.6 ± 3.8	23.0 ± 0.8	15.7 ± 6.5	0.61 ± 0.15	10.5 ± 7.7
helix B	0.92 ± 0.03	13.0 ± 3.0		13.0 ± 3.0	0.47 ± 0.11	5.8 ± 2.6
helix C	0.92 ± 0.03	12.8 ± 3.1		12.8 ± 3.1	0.65 ± 0.18	8.5 ± 4.3
helix D	0.93 ± 0.03	11.8 ± 2.9	17.8	12.4 ± 3.9	0.56 ± 0.10	5.6 ± 3.3
β-sheet	0.86 ± 0.10	16.7 ± 7.4		16.7 ± 7.4	0.55 ± 0.10	13.8 ± 8.3
N-terminal	0.56 ± 0.33	26.8 ± 6.2	53.9	40.3 ± 25.2	2.07 ± 0.52	58.4 ± 9.2
C-terminal	0.60 ± 0.24	23.1 ± 5.1	51.2 ± 0.6	35.8 ± 17.0	1.79 ± 0.87	53.3 ± 8.7
AB1	0.78 ± 0.14	15.4 ± 5.1	32.1 ± 3.4	24.6 ± 12.3	0.71 ± 0.08	16.0 ± 6.4
AB2	0.65 ± 0.21	21.4 ± 5.8	37.4 ± 11.9	34.5 ± 15.6	1.19 ± 0.60	24.9 ± 14.2
BC	0.87 ± 0.07	16.8 ± 5.1		16.8 ± 5.1	1.20 ± 0.44	29.5 ± 9.5
CD	0.73 ± 0.12	21.9 ± 5.3	29.7 ± 4.4	28.1 ± 10.3	1.08 ± 0.22	33.4 ± 18.2

[a] The overall amplitude of the angular fluctuations observed for a particular N–H vector is estimated to be $0.5\phi_s + \theta_0$, where ϕ_s is the angle defining a two-site jump and θ_0 is the semiangle defining diffusion in a cone. In cases where only a single fast motion is needed to model the fluctuations, $\phi_s = 0$. [b] The rmsd is calculated for the backbone nitrogen atoms of each of ten structures relative to the average structure when the backbone atoms of residues 3–127 are superimposed to give a best fit. [c] Θ_{av} is the average angle between the N–H vector in each of ten calculated solution structures and the N–H vector in the average solution structure. [d] Helices A, B, C, and D contain residues 5–17, 41–57, 72–90, and 110–125, respectively. Residue 109 bridges the β-strand (106–108) and helix D; here it is included in helix D rather than introducing an additional loop containing only one residue. The β-sheet contains residues 28–30 and 106–108. The N- and C-termini contain residues 3–4 and 126–129, respectively. The AB1, AB2, BC, and CD loops contain residues 18–27, 31–40, 58–71, and 91–105, respectively. [e] The values given are the average ± one standard deviation.

some of the smallest values of S^2 found in the protein; indicating that these residues are undergoing significant motion on a time scale faster than the rotational correlation time. Closely similar behavior has been observed for the terminal regions of other proteins including staphylococcal nuclease, interleukin-1β, ubiquitin, and glucose permease IIA domain (Kay et al., 1989; Clore et al., 1990b; Schneider et al., 1992; Stone et al., 1992). It is interesting in IL-4 that this motional behavior occurs even though the N- and C-termini are linked by a disulfide bridge (3–127). The motions of the N- and C-termini do not appear to be highly correlated; no NOE effects between residues 0–2 and 128–129 are seen in NOESY spectra.

Both the AB and the CD loops, which run the length of the helix bundle, give S^2 values that are significantly smaller than those observed for the regions of secondary structure. These two loops interact through the short region of the irregular antiparallel β-sheet involving residues 28–30 in the center of the AB loop and residues 106–108 at the end of the CD loop. This short region of β-sheet divides the AB loop into two segments of equal length, denoted AB1 and AB2. The AB2 loop has the lowest S^2 value of these three regions while the AB1 loop has the highest S^2 value. The observed average order parameter for the BC loop of 0.87, however, is significantly higher than that observed for the other loops and is only slightly lower than that observed for regions of regular secondary structure.

The values of S^2 are sensitive to motions faster than the rotational correlation time and follow closely the value of the NOEs. T_2 values are, however, influenced by events on slower time scales and most notably by chemical-exchange effects. Conformational fluctuations on the millisecond time scale, for example, may generate such effects, causing a decrease in T_2. This can be detected by T_1/T_2 ratios which are larger than anticipated from the overall correlation time. There are 17 residues in IL-4 with T_1/T_2 ratios significantly above 5.2, for which an exchange contribution to the line width (Δex) of more than 0.5 Hz is required. It is striking that all these residues are located close to either the 24–65 or 46–99 disulfide bridges or to the β-sheet region as shown in Figure 2; the presence of the covalent S–S bond or the β-sheet hydrogen bonds may serve to slow the motions of these residues, bringing them into the time-scale range where exchange effects may be seen. Some of these residues (22, 24, 99, 103, 104) correspond to loop regions where large amplitude subnano-

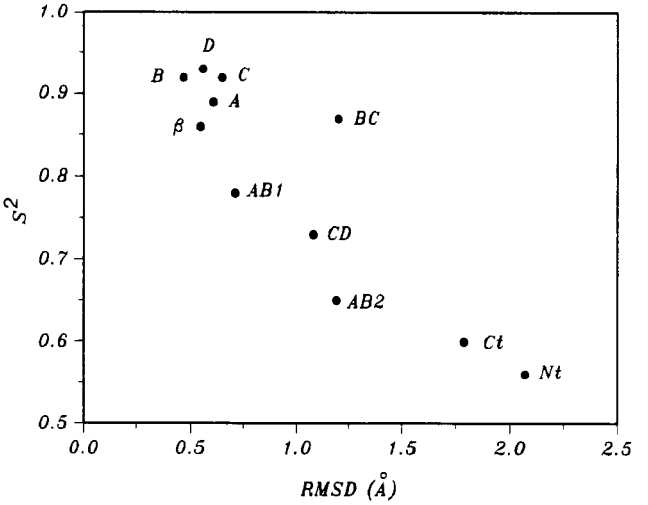

FIGURE 3: Plot of the average order parameter S^2 versus the average rmsd for the various structural regions of IL-4. Labels A, B, C, and D refer to the four helices, AB1, AB2, BC, and CD refer to the loop regions, and Nt and Ct refer to the N- and C-termini.

second motions have also been detected whereas the others correspond to regions where this is not the case. The latter include residues of the BC loop (59–61, 63, and 67); this suggests that slow motions may exist even if the fast fluctuations characteristic of the other loops are not occurring in this region.

The rmsd values for the backbone nitrogen atoms in the family of calculated NMR structures of IL-4 are shown in Figure 2E. It is immediately evident that there is a correlation between these values and the S^2 values; this is shown more directly in Figure 3. The observation of low S^2 values for the N- and C-termini and for the AB1, AB2, and CD loops suggests that the poor definition of these regions in the calculated structures, as reflected by large rmsd values, does arise from the dynamic behavior in these regions rather than simply a lack of assigned NOE effects. It is interesting that one region, the BC loop, deviates particularly noticeably from this general trend. Despite its high average S^2 value, this region has a high average rmsd value (1.20 Å), higher, in fact, than that of the AB1 and CD loops. The possible significance of this observation will be discussed below.

The rmsd values within the family of structures provide one measure of the degree of definition of different regions of the

calculated structure of IL-4. A second measure of the degree of structural definition is provided by the angular variation of the N–H vectors among the family of calculated structures (Θ_{av}), summarized in Table II for the different structural regions of IL-4. The smallest values of Θ_{av} are observed for the helical and β-sheet regions; values of less than 10° are observed for the majority of residues in these regions. Larger values of Θ_{av} are observed in the loop regions; angles varying between 7° and 62° are seen in the AB, BC, and CD loops. The largest values of Θ_{av} are found for the N- and C-termini where angles of greater than 40° are found for all residues.

The amplitude of angular fluctuations of individual N–H vectors, implied by the S^2 values, can be calculated using a fast diffusion in a cone model (Lipari & Szabo, 1980, 1981). This model can also be used to interpret the fast time-scale motions, defined by S^2_f, in the extended model of Clore et al. (1990a). The angular fluctuations on the slower time scale, implied by S^2_s, can be interpreted in terms of a two-site jump model with equal populations (Wittebort & Szabo, 1978; Clore et al., 1990a). Values of the semiangle θ_0, derived from the diffusion in a cone model, and of ϕ_s derived from the two-site jump model, are summarized in Table II for the various structural regions of IL-4. Within the helical core of the protein fast fluctuations involve semiangles of approximately 13 ±3°, indicating restricted motion. The semiangles calculated for the loop regions are somewhat higher than those seen in the regions of regular secondary structure with values above 25° observed for several residues. The largest values of θ_0 are observed for the N- and C-termini; however, these values are not found to exceed 32°. Nearly all of the residues (20 of 23) whose relaxation data have been analyzed using the extended model of Clore et al. (1990a) are located in the loop regions and the N- and C-termini. For the residues in the AB1, AB2, and CD loops, values of ϕ_s, the angle defining the two-site jump, range from 24° to 56°. For the N- and C-termini values of greater than 50° are found. Three of the 23 residues analyzed using the extended model are located at the beginning of helix A and the end of helix D; these residues have ϕ_s values of approximately 20°. The overall amplitude of the angular fluctuations observed for a particular N–H vector when the extended model is applied can be estimated to be $0.5\phi_s + \theta_0$; in the case of the simpler models, the overall amplitude is θ_0, since ϕ is 0. It can be seen from Table II that the overall amplitude of motion of the N–H vector ($0.5\phi_s + \theta_0$) varies over a larger range of angles than the semiangle θ_0 and is significantly higher for the N- and C-termini and the AB1, AB2, and CD loops than for the helical core of the protein.

Despite the generally good correlation between S^2 and the rmsd of the solution structures, one region, the BC loop, is significantly more disordered in the calculated structures than the S^2 values would suggest. This could be because the conformational disorder involves fluctuations on a slower time scale than those that contribute to S^2, but it could also be that the high rmsd values conceal some structural preference in this loop region. In the BC loop, $\alpha N(i,i+3)$and $\alpha\beta(i,i+3)$ NOE effects involving residues T63 and L66 indicate a possible helical turn. Indeed, such a turn has been postulated by Garrett et al. (1992) on the basis of similar NOE effects and $^{13}C^{\alpha}$ secondary chemical shifts. The measured NH–αCH coupling constant of 8.5 Hz for C65 is not, however, consistent with such a helical turn. The BC loop is connected to the AB1 loop by the 24–65 disulfide bridge. However, there are only two NOE effects observed between these loops (G67–L23 and A68–L23). Several other residues in the BC loop give long-range NOE's to other parts of the protein, particularly helix C (H59–L27, H59–L109, E60–I80, L66–F73, T69–R75). These long-range NOE effects are not, however, sufficient to define a unique conformation for the BC loop or to define a unique orientation of the loop relative to the well-defined helix-bundle core. One possible reason for the difficulty in identifying sufficient long-range NOE's for this loop is the particularly large line widths for several residues (59–61, 63, 67) associated with exchange processes described above. Further analysis of the NMR data for these residues is required in order to determine the conformational properties of the BC loop.

The S^2 values for the AB and CD loops indicate motions of significant amplitude on a time scale faster than τ_R. The calculated solution structures of IL-4 show no well-defined structure in either of these loops. Examination of the NOE patterns and coupling constant values for the loop regions indicates, however, that these are far from expected for random structures. In all the loops NOE effects exist which could be characteristic of helical turns, but the NH–αCH coupling constants and chemical shifts are not consistent with this. For example, residues in the AB2 loop give a number of $\alpha N(i,i+3)$ and $\alpha N(i,i+4)$ NOE effects, but coupling constants in the range of 6.5–8.0 Hz, not characteristic of helical structure, are observed for residues 31, 33, 35, 36, and 38–40. Most of the 23 residues whose relaxation data have been analyzed using the extended form of the correlation function (Clore et al., 1990a) are located at the N- and C-termini and in the AB and CD loops (Table I). This dynamical model contains two rapid motions faster than τ_R, one very fast motion ($\tau_f \leq 10$ ps) characterized by an order parameter S^2_f, and one somewhat slower motion ($\tau_s \simeq 1$ ns) characterized by S^2_s. The AB and CD loops give τ_s values in the range of 0.5–3.2 ns and S^2_s values of 0.49–0.87 using this model; the S^2_s values correspond to ϕ_s angles of 25–56° using a two-site jump model with equal populations. It is interesting that all residues in the AB and CD loops which show motions on the 0.5–3.2-ns time scale themselves have or neighbor a residue with an NH–αCH coupling constant which is characteristic of conformational averaging (6.5–8.0 Hz). Thus, this motion may reflect a change in one or more backbone torsion angles, which leads to an averaging of NMR parameters including NH–αCH coupling constants, chemical shifts, and NOE effects.

The observation of fast motions of significant amplitude in the loop regions of IL-4 may have important implications for protein structure calculations. It is interesting to speculate that some of the contributing conformers to the averaged structures may have helical content, while others do not; on the time average of the NMR experiment this would result in a set of NMR parameters which were not appropriate for a single ordered conformation. Additional structure calculations have been carried out on IL-4 in which the NMR restraints for the AB2 loop have been changed. If the short-range $(i,i+2)$, $(i,i+3)$, and $(i,i+4)$ NOEs for residues 31–40 are removed, then the rmsd for the AB2 loop increases significantly compared to previous calculations without, however, increasing the rmsd of the four-helix-bundle core. If these NOE restraints are included and additional helical ϕ restraints are introduced for residues 31–40, then the AB2 loop is found to have helical turns and a much smaller rmsd value. Again the structural changes occur without disrupting the helix-bundle core. The conformational space sampled by the AB2 loop of IL-4 in solution may well be described best by structures taken from both of these additional structure calculation procedures. Preliminary structure calculations

have in fact shown that all the other loops are sufficiently long so to be able to have some helical character without disturbing the four-helix bundle at the core of the structure.

The issue of the ordering or otherwise of the loops is of particular significance in terms of crystallographic information on other helix-bundle proteins. In the crystal structure of GM-CSF high thermal parameters were identified for the two parts of the AB loop (Diederichs et al., 1991). Such high values were not evident for the CD loop, found to be flexible in interleukin-4. This does not necessarily mean that the two proteins differ; it is possible that the intermolecular contacts in the crystal are responsible for some diminution of flexibility in certain regions. Furthermore, it has been suggested (Bazan, 1992) that the crystal structure of IL-2 could be reinterpreted in terms of a structure much closer to IL-4 and GM-CSF than originally proposed (Brandhuber et al., 1987). Indeed, there is experimental NMR evidence that such similarity exists (Mott et al., 1992). A possible explanation for the difficulty in interpreting the crystal electron density map is that the loop dynamics make the chain trace indistinct in these regions.

Recent crystallographic results on the 1:2 complex of human growth hormone with its receptor indicate that both helical and loop regions of the four-helix-bundle topology are involved in binding (De Vos et al., 1992). Two of the human growth hormone loops have short regions of helical structure in the complex which are not evident in the crystal structure of uncomplexed porcine growth hormone (De Vos et al., 1992; Abdel-Meguid et al., 1987). Whether or not these are induced on binding, rather than being intrinsic to the four-helix bundle of human growth hormone, must await more detailed structural analysis. Few details of the receptor binding regions in interleukin-4 are currently available. It seems likely, however, that the conformational disorder of the loop regions of the IL-4 molecule observed in this study would be reduced if such regions are involved in binding to the receptor and that the "nascent" structure detected in the unbound molecule might thereby become well-defined.

ACKNOWLEDGMENT

We are most grateful to G. M. P. Lawrence, R. G. Edwards, and C. Gershter for the labeled IL-4 used in these studies, and we thank B. Weston, S. Box, J. M. Dewdney, and D. V. Gardner for their support and encouragement.

SUPPLEMENTARY MATERIAL AVAILABLE

A table containing experimental and calculated T_1, T_2, and NOE values along with the calculated S^2, S^2_s, S^2_f, τ_e, τ_s, and $\pi\Delta$ex parameters (8 pages). Ordering information is given on any current masthead page.

REFERENCES

Abdel-Meguid, S. S., Shiel, H.-S., Smith, W. W., Dayringer, H. E., Violand, B. N., & Bentle, L. A. (1987) *Proc. Natl. Acad. Sci. U.S.A. 84*, 6434–6437.

Abragam, A. (1961) *Principles of Nuclear Magnetism*, Oxford University Press, London.

Barbato, G., Ikura, M., Kay, L. E., Pastor, R. W., & Bax, A. (1992) *Biochemistry 31*, 5269–5278.

Bazan, J. F. (1992) *Science 257*, 410–412.

Bodenhausen, G., & Ruben, D. (1980) *Chem. Phys. Lett. 69*, 185–189.

Boyd, J., Hommel, U., & Campbell, I. D. (1990) *Chem. Phys. Lett. 175*, 477–482.

Boyd, J., Hommel, U., & Krishnan, V. V. (1991) *Chem. Phys. Lett. 187*, 317–324.

Brandhuber, B. J., Boone, T., Kenney, W. C., & McKay, D. B. (1987) *Science 238*, 1707–1709.

Clore, G. M., Szabo, A., Bax, A., Kay, L. E., Driscoll, P. C., & Gronenborn, A. M. (1990a) *J. Am. Chem. Soc. 112*, 4989–4991.

Clore, G. M., Driscoll, P. C., Wingfield, P. T., & Gronenborn, A. M. (1990b) *Biochemistry 29*, 7387–7401.

De France, T., Vanbervliet, B., Aubrey, J. P., Takebe, Y., Arai, N., Miyajima, A., Yokota, T., Lee, F., Arai, K., de Vries, J. E., & Banchereau, J. (1987a) *J. Immunol. 139*, 1135–1141.

De France, T., Aubrey, J. P., Rousset, F., Vanbervliet, B., Bonnefoy, J. Y., Arai, N., Takebe, Y., Yokota, T., Lee, F., de Vries, J. E., & Banchereau, J. (1987b) *J. Exp. Med. 165*, 1459–1467.

De Vos, A. M., Ultsch, M., & Kossiakoff, A. A. (1992) *Science 255*, 306–312.

Diederichs, K., Boone, T., & Karplus, P. A. (1991) *Science 254*, 1779–1782.

Garrett, D. S., Powers, R., March, C. J., Frieden, E. A., Clore, G. M., & Gronenborn, A. M. (1992) *Biochemistry 31*, 4347–4353.

Hiyama, Y., Niu, C., Silverton, J. V., Bavoso, A., & Torchia, D. A. (1988) *J. Am. Chem. Soc. 110*, 2378.

Howard, M., Farrar, J., Hilfiker, M., Johnson, B., Takatsu, K., Hamaoka, T., & Paul, W. E. (1982) *J. Exp. Med. 155*, 914–923.

Kay, L. E., Torchia, D. A., & Bax, A. (1989) *Biochemistry 28*, 8972–8979.

Kay, L. E., Nicholson, L. K., Delaglio, F., Bax, A., & Torchia, D. A. (1992) *J. Magn. Reson. 97*, 359–375.

Keiter, E. A. (1986) Ph.D. Thesis, University of Illinois.

Kördel, J., Skelton, N. J., Akke, M., Palmer, A. G., III, & Chazin, W. J. (1992) *Biochemistry 31*, 4856–4866.

Kraulis, P. (1991) *J. Appl. Crystallogr. 24*, 946–950.

Lipari, G., & Szabo, A. (1980) *Biophys. J. 30*, 489–506.

Lipari, G., & Szabo, A. (1981) *J. Chem. Phys. 75*, 2971–2976.

Lipari, G., & Szabo, A. (1982a) *J. Am. Chem. Soc. 104*, 4546–4559.

Lipari, G., & Szabo, A. (1982b) *J. Am. Chem. Soc. 104*, 4559–4570.

Messerle, B. A., Wider, G., Otting, G., Weber, C., & Wüthrich, K. (1989) *J. Magn. Reson. 85*, 608–613.

Mott, H. R., Driscoll, P. C., Boyd, J., Cooke, R. M., Weir, M. P., & Campbell, I. D. (1992) *Biochemistry 31*, 7741–7744.

Oas, T. G., Hartzell, C. J., Dalquist, F. W., & Drobny, G. P. (1987) *J. Am. Chem. Soc. 109*, 5962.

Olejniczak, E. T., Dobson, C. M., Karplus, M., & Levy, R. M. (1984) *J. Am. Chem. Soc. 106*, 1923–1930.

Palmer, A. G., Skelton, N. J., Chazin, W. J., Wright, P. E., & Rance, M. (1992) *Mol. Phys. 75*, 699–711.

Powers, R., Garrett, D. S., March, C. J., Frieden, E. A., Gronenborn, A. M., & Clore, G. M. (1992) *Science 256*, 1673–1677.

Redfield, C., Smith, L. J., Boyd, J., Lawrence, G. M. P., Edwards, R. G., Smith, R. A. G., & Dobson, C. M. (1991) *Biochemistry 30*, 11029–11035.

Schneider, D. M., Dellwo, M. J., & Wand, A. J. (1992) *Biochemistry 31*, 3645–3652.

Shoji, A., Ozaki, T., Fujito, T., Deguchi, K., Ando, S., & Ando, I. (1990) *J. Am. Chem. Soc. 112*, 4693–4697.

Smith, L. J., Redfield, C., Boyd, J., Lawrence, G. M. P., Edwards, R. G., Smith, R. A. G., & Dobson, C. M. (1992) *J. Mol. Biol. 224*, 899–904.

States, D. J., Haberkorn, R. A., & Ruben, D. J. (1982) *J. Magn. Reson. 48*, 286–292.

Stone, M. J., Fairbrother, W. J., Palmer, A. G., Reizer, J., Saier, M., & Wright, P. E. (1992) *Biochemistry 31*, 4394–4406.

Vercelli, D., Jabara, H. H., Arai, K.-I., & Geha, R. S. (1989) *J. Exp. Med. 169*, 1295–1307.

Wittebort, R. J., & Szabo, A. (1978) *J. Chem. Phys. 69*, 1722–1736.